Designing Fresnel microlenses for focusing astigmatic multi-Gaussian beams by using fractional order Fourier transforms

Journal of Physics: Conference Series **274** (2011) 012108 doi:10.1088/1742-6596/274/1/012108

Designing Fresnel microlenses for focusing astigmatic multi-Gaussian beams by using fractional order Fourier transforms

A Patiño[1,2], P-E Durand[2], É Fogret[2] and P Pellat-Finet[2]

[1] Universidad Technológica de Bolivar, Cartagena de Indias, Colombia
[2] Laboratoire de mathématiques et applications des mathématiques, Université de Bretagne Sud, B P 92116, 56321 Lorient cedex, France

E-mail: alberto.patino-vanegas@univ-ubs.fr

Abstract. According to a scalar theory of diffraction, light propagation can be expressed by two-dimensional fractional order Fourier transforms. Since the fractional Fourier transform of a chirp function is a Dirac distribution, focusing a light beam is optically achieved by using a diffractive screen whose transmission function is a two–dimensional chirp function. This property is applied to designing Fresnel microlenses, and the orders of the involved Fourier fractional transforms depend on diffraction distances as well as on emitter and receiver radii of curvature. If the emitter is astigmatic (with two principal radii of curvature), the diffraction phenomenon involves two one-dimensional fractional Fourier transforms whose orders are different. This degree of freedom allows us to design microlenses that can focus astigmatic Gaussian beams, as produced by a line-shaped laser diode source.

1. Introduction

Laser microtooling makes use of more and more powerful laser diodes for obtaining mechanical effects on various materials for a lot of applications. Anyway, in many cases it can be useful to gather several laser diodes to increase the focus irradiance. Figure 1 shows a light source made up of 19 aligned laser diodes; the whole device is about 2 cm long. Each laser diode is about 0.5 mm long and 0.25 mm wide (we own such a source at $\lambda = 0.808\,\mu$m). The problem to solve is twofold:

(i) How to focus all the sources on a common area?

(ii) The considered laser diodes emit Gaussian beams whose waists are elliptical, so that beam divergences along two orthogonal directions are different from each other. When imaged through a lens, these Gaussian beams become astigmatic, in the sense that they are focused on two orthogonal segments at different distances. We have to design sphero-cylindrical lenses that compensate this effect.

Several solutions to the former technical problem have been proposed: beam shaping technique based on rectangular cubes and stripe-mirror plates [1]; array of multi-prisms [2]; two mirror beam shaping [3].

Diffractive computed elements have the advantage of providing solutions of the two above mentioned points at once. They are generally compact and can be produced with high qualities;

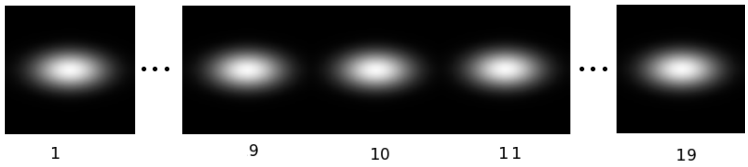

Figure 1. A source made up of 19 laser diodes, as used for microtooling. Each diode produces an astigmatic Gaussian beam whose waist is elliptical, as shown in the figure.

they also can be combined with refractive elements in hybrid systems [4]. They can be used to solve problems similar to the above mentioned one [5, 6].

In this paper, we explain how to design Fresnel microlenses that provide solutions for the considered problem. First, we design spherical diffractive lenses, able to focus a plane wave on a given off axis point at a given distance. Such a lens can be considered as introducing a spatial chirp function and the analysis is developed in the framework of fractional Fourier optics [7, 8, 9]. Then we examine the problem of focusing an astigmatic Gaussian beam on a plane surface. Expressing Fresnel diffraction with the help of fractional Fourier transforms has the advantage of splitting the analysis in two parts, dealing with one-dimensional transforms that can be adapted to orthogonal directions. Finally, since we consider microlenses, we choose to set a lens in front of each of the 19 laser diodes; each lens is appropriately shifted.

2. Background theories and results

2.1. The fractional order Fourier transform

With Cartesian coordinates, if $\boldsymbol{\rho} = (\xi, \eta)$, we denote $\rho = (\xi^2 + \eta^2)^{1/2}$ and $\mathrm{d}\boldsymbol{\rho} = \mathrm{d}\xi\,\mathrm{d}\eta$. Then, according to Namias [10, 11], we define the two-dimensional Fourier transform of order α of function f by

$$\mathcal{F}_\alpha[f](\boldsymbol{\sigma}) = \frac{\mathrm{i}\mathrm{e}^{-\mathrm{i}\alpha}}{\sin\alpha}\exp[-\mathrm{i}\pi\sigma^2\cot\alpha]\int_{\mathbb{R}^2}\exp[-\mathrm{i}\pi\rho^2\cot\alpha]\exp\left[\frac{2\mathrm{i}\pi\boldsymbol{\rho}\cdot\boldsymbol{\sigma}}{\sin\alpha}\right]f(\boldsymbol{\rho})\,\mathrm{d}\boldsymbol{\rho}\,, \tag{1}$$

where $\boldsymbol{\rho}\cdot\boldsymbol{\sigma}$ denotes the Euclidean scalar product of $\boldsymbol{\rho}$ and $\boldsymbol{\sigma}$. (Generally α is a complex number [10, 11], although in this paper we consider real α only.)

The usual Fourier transform is obtained for $\alpha = \pi/2$. The operator $\mathcal{F}_0$ is the identity operator. Fractional order Fourier transforms compose according to

$$\mathcal{F}_\alpha \circ \mathcal{F}_\beta = \mathcal{F}_{\alpha+\beta}\,. \tag{2}$$

In this paper, we also use the one-dimensional fractional Fourier transform, defined by

$$\mathcal{F}^{[1]}_\alpha[f](\xi') = \frac{\mathrm{e}^{\mathrm{i}\mathfrak{s}(\alpha)\pi/4}\,\mathrm{e}^{-\mathrm{i}\alpha/2}}{\sqrt{|\sin\alpha|}}\,\mathrm{e}^{-\mathrm{i}\pi\xi'^2\cot\alpha}\int_{\mathbb{R}}\mathrm{e}^{-\mathrm{i}\pi\xi^2\cot\alpha}\,\exp\left[\frac{2\mathrm{i}\pi\xi\xi'}{\sin\alpha}\right]\,f(\xi)\,\mathrm{d}\xi\,, \tag{3}$$

where $\mathfrak{s}(\alpha)$ is the sign of α. According to Fubini theorem, if f is a two-dimensional function, we have

$$\mathcal{F}_\alpha[f](\xi', \eta') = \mathcal{F}^{[1]}_\alpha\Big[\mathcal{F}^{[1]}_\alpha[f_\eta](\xi')\Big](\eta')\,, \tag{4}$$

where f_η is defined for every η by

$$f_\eta(\xi) = f(\xi, \eta)\,. \tag{5}$$

Eq. (2) holds true for one-dimensional fractional order Fourier transforms.

2.2. Fresnel diffraction as a fractional Fourier transform

We shortly recall some results of fractional Fourier optics [7, 8, 9]. Let $\mathcal{A}$ be a monochromatic spherical emitter whose radius of curvature is R_A and wavelength is λ (radius is taken from vertex to center of curvature); let $\mathcal{B}$ be a spherical receiver (radius R_B) at a distance D. We choose coordinates $\boldsymbol{r} = (x, y)$ on $\mathcal{A}$ and $\boldsymbol{s}$ on $\mathcal{B}$. According to a scalar theory of difraction, the field amplitude U_B on $\mathcal{B}$ is deduced from the field amplitude U_A on $\mathcal{A}$ by [7, 8, 9, 12, 13]

$$U_B(\boldsymbol{s}) = \frac{\mathrm{i}}{\lambda D} \exp\left[-\frac{\mathrm{i}\pi}{\lambda}\left(\frac{1}{R_B}+\frac{1}{D}\right)s^2\right] \int_{\mathbb{R}^2} \exp\left[-\frac{\mathrm{i}\pi}{\lambda}\left(\frac{1}{D}-\frac{1}{R_A}\right)r^2\right] \exp\left[\frac{2\mathrm{i}\pi}{\lambda D}\boldsymbol{s}\cdot\boldsymbol{r}\right] U_A(\boldsymbol{r})\,\mathrm{d}\boldsymbol{r}\,, \tag{6}$$

where a constant factor $\exp[-2\mathrm{i}\pi D/\lambda]$ has been omitted.

For expressing Eq. (6) as a fractional order Fourier transform, we introduce an auxiliary parameter ε such that $\varepsilon R_A > 0$ and

$$\varepsilon^2 = \frac{D(D+R_B)}{(R_A-D)(D-R_A+R_B)}\,, \tag{7}$$

and choose $\alpha \in]-\pi, \pi[$, such that $\alpha D \geq 0$ and

$$\cot^2\alpha = \frac{(D+R_B)(R_A-D)}{D(D-R_A+R_B)}\,. \tag{8}$$

We use scaled variables

$$\boldsymbol{\rho} = \frac{\boldsymbol{r}}{\sqrt{\lambda\varepsilon R_A}}\,, \qquad\qquad \boldsymbol{\sigma} = (\cos\alpha + \varepsilon\sin\alpha)\frac{\boldsymbol{s}}{\sqrt{\lambda\varepsilon R_A}}\,, \tag{9}$$

and scaled field amplitudes

$$V_A(\boldsymbol{\rho}) = U_A\left(\sqrt{\lambda\varepsilon R_A}\,\boldsymbol{\rho}\right)\,, \qquad\qquad V_B(\boldsymbol{\sigma}) = U_B\left(\frac{\sqrt{\lambda\varepsilon R_A}\,\boldsymbol{\sigma}}{\cos\alpha+\varepsilon\sin\alpha}\right)\,. \tag{10}$$

Finally, Eq. (6) becomes

$$V_B(\boldsymbol{\sigma}) = \mathrm{e}^{\mathrm{i}\alpha}(\cos\alpha+\varepsilon\sin\alpha)\mathcal{F}_\alpha[V_A](\boldsymbol{\sigma})\,. \tag{11}$$

Eq. (11) means that the field transfer by diffraction from an arbitrary emitter to an arbitrary receiver can be expressed by a fractional order Fourier transform.

So far, both α and ε have been implicitly assumed to be real numbers. A generalization to complex values is sometimes necessary [8, 14].

Finally, we point out that Eqs. (7) and (8) still stand for a plane receiver ($R_B \to \infty$): then

$$\cot^2\alpha = \frac{R_A - D}{D}\,. \tag{12}$$

2.3. Chirp functions, their fractional Fourier transforms and their interpretation in optics

Let $\delta_{\boldsymbol{\rho}_0} = \delta(\boldsymbol{\rho}-\boldsymbol{\rho}_0)$ denote the Dirac distribution (or generalized function) whose support is $\{\boldsymbol{\rho}_0\}$. According to Namias [10], we have

$$\mathcal{F}_\alpha[\delta_{\boldsymbol{\rho}_0}](\boldsymbol{\sigma}) = \frac{\mathrm{i}\mathrm{e}^{-\mathrm{i}\alpha}}{\sin\alpha}\exp\left[-\mathrm{i}\pi(\sigma^2+\rho_0^2)\cot\alpha + \frac{2\mathrm{i}\pi\boldsymbol{\sigma}\cdot\boldsymbol{\rho}_0}{\sin\alpha}\right] = -\Gamma_{-\alpha,\boldsymbol{\rho}_0}(\boldsymbol{\sigma})\,, \tag{13}$$

and $\Gamma_{\alpha,\boldsymbol{\rho}_0}$ will be called a scaled chirp function.

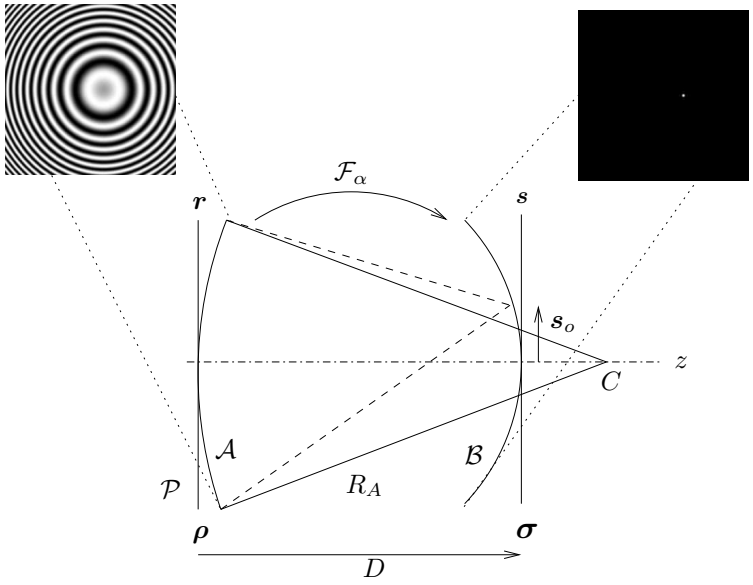

Figure 2. Top left: complex amplitude on emitter $\mathcal{A}$, corresponding to the phase of a Fresnel lens (represented by grey levels). Top right: corresponding focus on receiver $\mathcal{B}$. The lens is not centred, so that the focus on $\mathcal{B}$ is shifted by $\boldsymbol{s}_0$. Parameters in the figure are spatial ones; scaled parameters are needed for actual simulations, according to Eq. (9).

By inverting the fractional Fourier transform in Eq. (13), we obtain

$$\delta(\boldsymbol{\sigma} - \boldsymbol{\sigma}_0) = \mathcal{F}_\alpha[\Gamma_{\alpha,\boldsymbol{\sigma}_0}](\boldsymbol{\sigma})\,. \tag{14}$$

Optically, Eq. (14) means that a chirp function represents the field amplitude of a converging wave: the focus is a luminous point whose amplitude is represented by a Dirac distribution. The result can be explicitely deduced by passing from scaled variables to spatial ones: $\Gamma_{\alpha,\boldsymbol{\sigma}_0}$ is seen like the scaled field amplitude on $\mathcal{A}$ corresponding to

$$U_A(\boldsymbol{r}) = \frac{\mathrm{i}\mathrm{e}^{\mathrm{i}\alpha}}{\sin\alpha} \exp\left[\frac{\mathrm{i}\pi}{\lambda\varepsilon R_A}\Big(r^2 + (\cos\alpha + \varepsilon\sin\alpha)s_0^2\Big)\cot\alpha - \frac{2\mathrm{i}\pi(\cos\alpha+\varepsilon\sin\alpha)}{\lambda\varepsilon R_A}\boldsymbol{s}_0\cdot\boldsymbol{r}\right]. \tag{15}$$

The field on $\mathcal{B}$ (radius R_B), at a distance D, is a luminous point, located at $\boldsymbol{s}_0$, provided that ε and α are chosen according to Eqs. (7) and (8). The situation is illustrated in Fig. 2.

We introduce the scaled function $G_{\alpha,a}$ such that

$$G_{\alpha,a}(\xi) = \frac{\mathrm{e}^{\mathrm{i}\mathfrak{s}(\alpha)\pi/4}\mathrm{e}^{-\mathrm{i}\alpha/2}}{\sqrt{|\sin\alpha|}} \exp\left[-\mathrm{i}\pi(\xi^2+a^2)\cot\alpha + \frac{2\mathrm{i}\pi a\xi}{\sin\alpha}\right], \tag{16}$$

so that the former scaled chirp functions Γ can be written

$$\Gamma_{\alpha,\boldsymbol{\rho}_0}(\boldsymbol{\sigma}) = \Gamma_{\alpha,\xi_0,\eta_0}(\xi,\eta) = G_{\alpha,\xi_0}(\xi)\,G_{\alpha,\eta_0}(\eta)\,. \tag{17}$$

We then define the function $C_{\alpha,a,R}$ by

$$\begin{aligned} C_{\alpha,a,R}(x) \;=\; & \frac{\mathrm{e}^{\mathrm{i}\mathfrak{s}(\alpha)\pi/4}\mathrm{e}^{-\mathrm{i}\alpha/2}}{\sqrt{|\sin\alpha|}} \exp\left[\frac{\mathrm{i}\pi}{\lambda\varepsilon R}\Big(x^2 + (\cos\alpha+\varepsilon\sin\alpha)a^2\Big)\cot\alpha\right] \\ & \times \exp\left[-\frac{2\mathrm{i}\pi(\cos\alpha+\varepsilon\sin\alpha)}{\lambda\varepsilon R}ax\right], \end{aligned} \tag{18}$$

so that Eq. (15) becomes

$$U_A(\boldsymbol{r}) = U_A(x,y) = C_{\alpha,x'_0,R_A}(x)\, C_{\alpha,y'_0,R_A}(y)\,, \tag{19}$$

whith $\boldsymbol{s}_0 = (x'_0, y'_0)$.

Functions $G_{\alpha,a}$ are scaled versions of functions $C_{\alpha,a,R}$. The one-dimensional fractional Fourier transform of order α of $G_{\alpha,a}$ is the Dirac distribution δ_a.

2.4. Fractional sampling

The Shannon–Whittaker sampling theorem is extended to the fractional domain as follows. A function is said to be α-bandlimited if its fractional Fourier transform of order α has a finite support. Let f be a α-bandlimited function: the support of its fractional Fourier transform of order α is included in $[-B/2, B/2]$. Then f can be exactly reconstructed from its sampled values $f(n \sin\alpha/B)$ according to [15]

$$f(\xi) = \mathrm{e}^{\mathrm{i}\pi\xi^2 \cot\alpha} \sum_n \mathrm{e}^{-\mathrm{i}\pi n^2 \sin\alpha\cos\alpha/B^2} f\left(\frac{n\sin\alpha}{B}\right) \frac{\sin\left(\dfrac{\pi B\xi}{\sin\alpha} - n\pi\right)}{\dfrac{\pi B\xi}{\sin\alpha} - n\pi}\,. \tag{20}$$

The sampling rate should be less than or equal to

$$\Delta\xi = \frac{\sin\alpha}{B}\,. \tag{21}$$

3. Design of Fresnel microlenses

3.1. Spherical microlenses

A Fresnel lens is obtained when the field on the emitter $\mathcal{A}$ is given by Eq. (15). Since holographic plates are plane, the lens will be built on a plane, say $\mathcal{P}$. The field amplitude on $\mathcal{P}$ is related to the amplitude on $\mathcal{A}$ by [9, 12, 13]

$$U_P(\boldsymbol{r}) = U_A(\boldsymbol{r})\, \exp\left[\frac{\mathrm{i}\pi}{\lambda R_A} r^2\right]\,, \tag{22}$$

where $U_A(\boldsymbol{r})$ is given by Eq. (15).

For the actual microlens computing we have to determine the sampling rate. We assume having $N_x\, N_y$ pixels on the diffractive element $\mathcal{P}$ (the Fresnel lens is related to x and y orthogonal axis), and $N'_x\, N'_y$ on the receiver $\mathcal{B}$. We assume $N'_x = N_y$ and $N'_y = N_y$. We denote $\Delta x\, \Delta y$ the pixel size on $\mathcal{A}$, and $\Delta x'\, \Delta y'$ on $\mathcal{B}$. We reason on x only: the corresponding scaled pixel on $\mathcal{P}$ is

$$\Delta\xi = \frac{\Delta x}{\sqrt{\lambda\varepsilon R_A}}\,. \tag{23}$$

According to Eq. (21), the support of the scaled field on $\mathcal{B}$ is $[-B_\xi/2, B_\xi/2]$ with

$$B_\xi = \frac{\sin\alpha}{\Delta\xi}\,, \tag{24}$$

so that the size of the scaled pixel on $\mathcal{B}$ is

$$\Delta\xi' = \frac{B_\xi}{N_x} = \frac{\sin\alpha}{N_x \Delta\xi}\,. \tag{25}$$

With spatial variables (x', y') on $\mathcal{B}$, the size of a pixel is $\Delta x'\, \Delta y'$ with

$$\Delta x' = \frac{\lambda\varepsilon R_A}{\cos\alpha + \varepsilon\sin\alpha}\, \frac{\sin\alpha}{N_x \Delta x}\,, \qquad \Delta y' = \frac{\lambda\varepsilon R_A}{\cos\alpha + \varepsilon\sin\alpha}\, \frac{\sin\alpha}{N_y \Delta y}\,. \tag{26}$$

3.2. Sphero-cylindrical microlenses

By comparison with Eqs. (15) and (22), the field corresponding to a sphero-cylindrical lens takes the form

$$U_P(x,y) = C_{\alpha_x,0,R_x}(x)\, C_{\alpha_y,0,R_y}(y)\, \exp\left[\frac{\mathrm{i}\pi}{\lambda R_x}x^2\right]\, \exp\left[\frac{\mathrm{i}\pi}{\lambda R_y}y^2\right]\,, \tag{27}$$

where R_x and R_y are the principal radii of curvature [16] of the sphero-cylindrical wave emerging from the lens (the lens is assumed to be illuminated by a plane wave). The orders α_x and α_y are computed according to Eq. (12) for a plane receiver. Explicitly

$$\cot^2\alpha_x = \frac{R_x - D_x}{D_x}\,, \qquad\qquad \cot^2\alpha_y = \frac{R_y - D_y}{D_y}\,, \tag{28}$$

where D_x (D_y) is the distance where the focus line parallel to the x-axis (y-axis) should be observed. In each case, parameters ε_x and ε_y are computed according to Eq. (7), and then scaled variables and scaled functions, according to Eqs. (9) and (10).

Using fractional order Fourier transforms allows us to separate variables in representing light propagation from an astigmatic surface, as it should be clear from Eq. (27).

An example is given in Fig. 3. The focal distances of the lens are $f'_x = D_x = 10\,\mathrm{mm}$, and $f'_y = D_y = 15\,\mathrm{mm}$. The wavelength is $\lambda = 0.808\,\mu\mathrm{m}$. The radii are $R_x = 20\,\mathrm{mm}$, and $R_y = 18,75\,\mathrm{mm}$. We have $\alpha_x = 0.7\,854$ ($\varepsilon_x = 1$) and $\alpha_y = 1.1\,071$ ($\varepsilon_y = 2$).

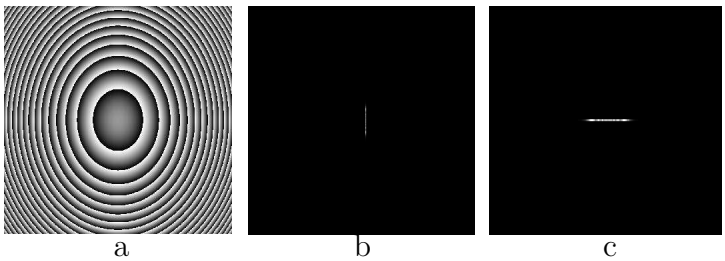

Figure 3. Design of a sphero-cylindrical Fresnel lens. (a) Complex amplitude on emitter $\mathcal{P}$, corresponding to the phase levels of the lens (represented by grey levels). (b) Focus line at distance 10 mm. (c) Focus line at distance 15 mm. (Numerical simulations.)

So far the lens was centred. Off axis focus lines centred at $x'_0 \neq 0$ for the one, and $y'_0 \neq 0$ for the other, are obtained by considering functions $C_{\alpha_x,x'_0,R_x}(x)$ and $C_{\alpha_y,y'_0,R_y}(y)$ in place of $C_{\alpha_x,0,R_x}(x)$ and $C_{\alpha_y,0,R_y}(y)$ in Eq. (27). Such lenses will be used in Sect. 4.4.

4. Focusing an astigmatic Gaussian beam

4.1. Cylindrical Gaussian beams

We recall some useful properties of Gaussian beams [9]. We consider a cylindrical Gaussian beam at wavelength λ and denote w_0 its waist (transverse) radius. At a distance d from the waist, the beam transverse radius is w_d such that

$$w_d{}^2 = w_0{}^2 + \frac{\lambda d^2}{\pi^2 w_0{}^2}\,, \tag{29}$$

and the radius of curvature of the wave surface is

$$R_d = -d - \frac{\pi^2 w_0{}^4}{\lambda^2 d}\,. \tag{30}$$

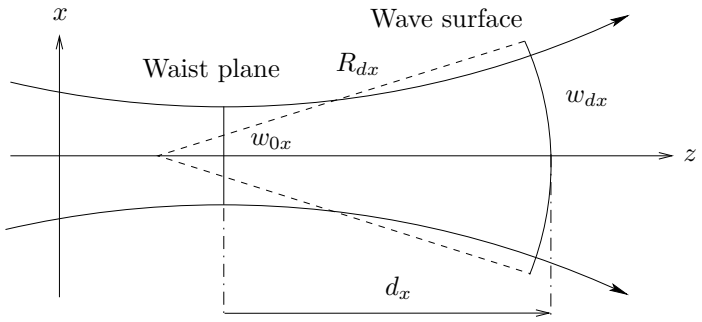

Figure 4. Gaussian beam parameters in the section of plane x–z. The direction of light propagation is z. The waist (tranverse) radius is w_{0x}. The principal curvature radius of the wave surface at a distance d_x is R_{dx}, and the transverse beam radius (along x) on this surface is w_{dx}. An equivalent diagram can be drawn in the orthogonal y–z section, with parameters w_{0y}, d_y, R_{dy} and w_{dy}. The Gaussian beam is astigmatic if $w_{0x} \neq w_{0y}$ or if $d_x \neq d_y$; then $R_{dx} \neq R_{dy}$ and $w_{dx} \neq w_{dy}$. The Gaussian beam is cylindrical if $w_{0x} = w_{0y}$ and $d_x = d_y$; then $R_{dx} = R_{dy}$ and $w_{dx} = w_{dy}$, and indices x and y are dropped.

These parameters are illustrated in Fig. 4.

We consider a lens transforming an incident Gaussian beam into an image Gaussian beam. We denote f' the image focal length of the lens. The waist of the object Gaussian beam is located on the lens axis, at W_0, and the waist of the image Gaussian beam at W_0' (generally, W_0' is not the paraxial image of W_0 [9]). If F is the object focus of the lens and F' its image focus, we denote $q = FW_0$ and $q' = F'W_0'$. Then we have [8, 9]

$$q' = \frac{-f'^2}{q + \dfrac{\pi^2 {w_0}^4}{\lambda^2 q}} \,. \tag{31}$$

The waist radius of the image beam is w_0' with

$${w_0'}^2 = \frac{f'^2 \lambda^2}{\pi^2 {w_0}^2} \, \frac{1}{1 + \dfrac{\lambda^2 q^2}{\pi^2 {w_0}^4}} \,. \tag{32}$$

4.2. Astigmatic Gaussian beams

4.2.1. Gaussian beam with elliptical waist. We apply the former results to astigmatic Gaussian beams. We consider a Gaussian beam whose waist is elliptical, with dimensions w_{0x} and w_{0y}. At a distance d, the wave surface has two principal curvature radii R_{dx} and R_{dy}, that is, according to Eq. (30)

$$R_{dx} = -d - \frac{\pi^2 {w_{0x}}^4}{\lambda^2 d} \,, \qquad\qquad R_{dy} = -d - \frac{\pi^2 {w_{0y}}^4}{\lambda^2 d} \,. \tag{33}$$

On this surface, according to Eq. (29), the beam area is (generally) an ellipse whose dimensions are w_{dx} and w_{dy} with

$${w_{dx}}^2 = w_{0x}^2 + \frac{\lambda d^2}{\pi^2 {w_{0x}}^2} \,, \qquad\qquad {w_{dy}}^2 = w_{0y}^2 + \frac{\lambda d^2}{\pi^2 {w_{0y}}^2} \,. \tag{34}$$

The diffraction from the elliptical waist to the wave surface at a distance d can be expressed as two one-dimensional fractional Fourier transforms — in the sense of Eq. (4) — whose orders are α_x and α_y, where the x and y directions are orthogonal to each other, and are along the principal sections of the wave surface [17]. The field amplitude, on the wave surface, corresponding to the fundamental mode, is written [9]

$$U_d(x,y) = U_0\sqrt{\frac{w_{0x}w_{0y}}{w_{dx}w_{dy}}}\,\exp\left[-\frac{x^2}{w_{dx}^2}-\frac{\mathrm{i}\pi d}{\lambda}+\frac{\mathrm{i}\alpha_x}{2}\right]\,\exp\left[-\frac{y^2}{w_{dy}^2}-\frac{\mathrm{i}\pi d}{\lambda}+\frac{\mathrm{i}\alpha_y}{2}\right], \qquad (35)$$

where U_0 is a dimensional constant.

4.2.2. Focusing an astigmatic Gaussian beam. We consider a Gaussian beam with elliptical waist. We deduce from Eq. (31) that a spherical lens focuses such a beam on two "focal" segments located at distances q'_x and q'_y from the image focus F', with

$$q'_x = \frac{-f'^2}{q+\dfrac{\pi^2 {w_{0x}}^4}{\lambda^2 q}}, \qquad q'_y = \frac{-f'^2}{q+\dfrac{\pi^2 {w_{0y}}^4}{\lambda^2 q}}. \qquad (36)$$

Indeed, these "focal" segments are one-dimensional waists, along the two principal directions x and y.

We now consider a sphero-cylindrical lens having two object foci F_x and F_y, two image foci F'_x and F'_y. The image focal lengths are f'_x and f'_y. Then Eqs. (36) are generalized according to

$$q'_x = \frac{-{f'_x}^2}{q_x+\dfrac{\pi^2 {w_{0x}}^4}{\lambda^2 q_x}}, \qquad q'_y = \frac{-{f'_y}^2}{q_y+\dfrac{\pi^2 {w_{0y}}^4}{\lambda^2 q_y}}, \qquad (37)$$

where $q_x = F_x W_0$, $q_y = F_y W_0$, $q'_x = F'_x W'_{0x}$, and $q'_y = F'_y W'_{0y}$ (W'_{0x} and W'_{0y} are where the focal segments intercept the optical axis).

4.2.3. General wave surface. When focused by a lens, an astigmatic Gaussian beam has two one-dimensional waists, located at different points on the optical axis, according to Eqs. (36) and (37). Then we have to consider a Gaussian beam with two waists. The former formulae can be applied if we use distances d_x and d_y in place of d, for example in Eqs. (33) and (34). Let $\mathcal{S}$ be a wave surface at a distance d_x from the x–waist and d_y from the y–waist. We generalize Eq. (35): the field amplitude on $\mathcal{S}$ is

$$U_S(x,y) = U_0\sqrt{\frac{w_{0x}w_{0y}}{w_{dx}w_{dy}}}\,\exp\left[-\frac{x^2}{w_{dx}^2}-\frac{\mathrm{i}\pi d_x}{\lambda}+\frac{\mathrm{i}\alpha_x}{2}\right]\,\exp\left[-\frac{y^2}{w_{dy}^2}-\frac{\mathrm{i}\pi d_y}{\lambda}+\frac{\mathrm{i}\alpha_y}{2}\right], \qquad (38)$$

where U_0 is a dimensional constant.

4.3. Optical setup

Before we give explicit results about the microlenses we have designed, we provide some features of the optical setup to be used in imaging the 19 laser diodes. The main point consists in using a refractive microlens in front of every laser diode. The reason is that each laser diode emits a Gaussian beam whose divergence angles overpass the capability of diffracted components, as produced nowadays. Numerical aperture of diffractive lenses is not sufficient for solving our problem with a unique diffractive element. Reducing the divergences is first obtained by using two refractive spherical microlenses (Fig. 5).

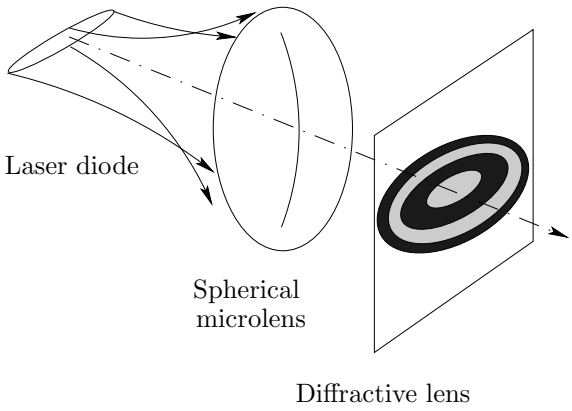

Figure 5. Optical set up for each one of the 19 laser diodes (see Fig. 1). The laser diode emits a Gaussian beam with elliptical waist. A spherical refractive microlens is set in front of the laser diode. The astigmatic Gaussian beam incident on the diffractive lens has two one-dimensional waists.

4.4. Designing a Fresnel lens for focusing an astigmatic Gaussian beam
We consider a Gaussian beam (with two waists), and a plane Fresnel lens at distances d_x and d_y from the waists. The complex amplitude of the field incident on the lens is

$$U_P(x,y) = U_S(x,y)\, \exp\left[\frac{\mathrm{i}\pi x^2}{\lambda R_x}\right] \exp\left[\frac{\mathrm{i}\pi y^2}{\lambda R_y}\right], \tag{39}$$

where $U_S(x,y)$ is given by Eq. (38), and where R_x and R_y have been obtained from Eq (33) after changing d into d_x and d_y.

We use the method of Sect. 3.2 and the following data:

$$\lambda = 0.808\,\mu\mathrm{m}\,, \quad w_{0x} = 341.74\,\mu\mathrm{m}\,, \quad w_{0y} = 176.47\,\mu\mathrm{m}\,, \quad d_x = 3\,\mathrm{mm}\,, \quad d_y = 4\,\mathrm{mm}\,.$$

In the first step we design a centred Fresnel lens that concentrates the luminous energy on an elliptical area, as shown in Fig. 6. The focal lengths of the lens are $f'_x = 40\,\mathrm{mm}$ and $f'_y = 7,2\,\mathrm{mm}$. The data of the image Gaussian beam (behind the diffractive lens) are

$$q'_x = -285.23\,\mu\mathrm{m}\,, \quad q'_y = -11.31\,\mu\mathrm{m}\,, \quad w'_{0x} = 30.00\,\mu\mathrm{m}\,, \quad w'_{0y} = 10.49\,\mu\mathrm{m}\,.$$

At a distance $z = 300\,\mathrm{mm}$ from the diffractive lens, we obtain an elliptical illuminated area (Fig. 6) with

$$w'_x = 2.23\,\mathrm{mm}\,, \quad w'_y = 7.18\,\mathrm{mm}\,.$$

These data hold for the field amplitude. If we consider the irradiance, the beam transverse radii are

$$W'_x = \frac{w'_x}{\sqrt{2}} = 1.58\,\mathrm{mm}\,, \quad W'_y = \frac{w'_y}{\sqrt{2}} = 5.08\,\mathrm{mm}\,.$$

We then consider the 19 laser diodes that constitute the luminous source to be imaged on a given area. The area is assumed to be almost a square area ($5{\times}5$ mm^2). The result is obtained by aligning side by side 19 elliptical luminous areas, identical to the one given in Fig. 6 c. For that purpose, the former centred lens in set in front of the central laser diode (number 10). Then we set a lens in front of every laser diode of the source: each lens is appropriately shifted. The shift is also calculated so that contiguous laser diodes will produce contiguous luminous areas. The result is illustrated in Fig. 7 (bottom right).

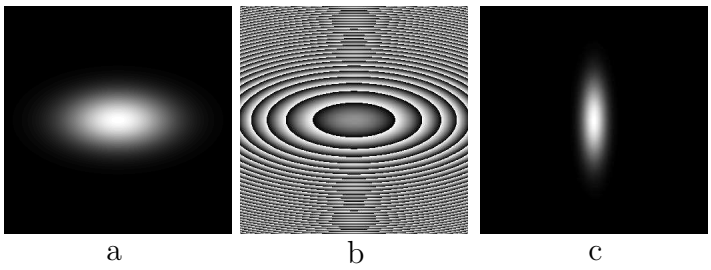

Figure 6. Focusing an astigmatic Gaussian beam on an elliptial area. (a) Gaussian beam irradiance in the lens plane. (b) Phase levels of the sphero-cylindrical Fresnel lens (represented by grey levels). (c) Irradiance at 30 mm from the lens. (Numerical simulations.)

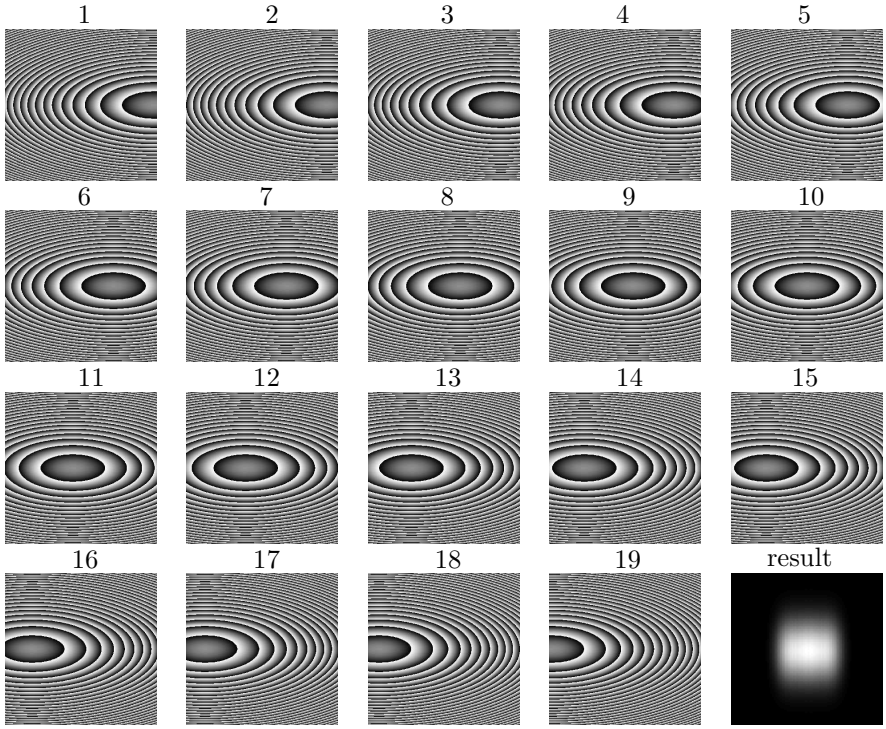

Figure 7. The 19 Fresnel lenses to be set in front of the 19 laser diodes. Each lens is appropriately shifted and produces an elliptical illuminated area, according to Fig. 6. Botton right: the resulting irradiance in the focus plane. For display convenience, the lenses are organized in an array: in fact they are aligned along a segment, as the laser diodes.

4.5. Another solution

This time we want to transform the elliptical waist into a circular illuminated area (radius about 10 mm). Intuitively we understand that between the two one-dimensional waists of an astigmatic Gaussian beam, there is a circular illuminated area. The situation is similar to the least diffusion circle that lies between the sagittal and tangential focal segments of a refractive lens, in presence of astigmatism.

The optical setup is that of Fig. 5 once more, so that the Gaussian beam incident on the diffractive lens is as in Sect. 4.4.

The location of the circular area, say $\mathcal{C}$, can be found as follows. Let C be the point where

the searched area intercepts the optical axis. Let W'_{0x} (W'_{0y}) be where the one-dimensional waist (radius w'_{0x}) along x (y) intercepts the optical axis. We denote $d'_x = W'_{0x}C$ and $d'_y = W'_{0y}C$. According to Eq. (29) — or (34) — the transverse beam radius along x on $\mathcal{C}$ is w'_{dx} with

$$w'^{\,2}_{dx} = w'^{\,2}_{0x} + \frac{\lambda^2 d'^{\,2}_x}{\pi^2 w'^{\,2}_{0x}}\,, \tag{40}$$

and the transverse beam radius along y on $\mathcal{C}$ is w'_{dy} with

$$w'^{\,2}_{dy} = w'^{\,2}_{0y} + \frac{\lambda^2 d'^{\,2}_y}{\pi^2 w'^{\,2}_{0y}}\,. \tag{41}$$

The illuminated area on $\mathcal{C}$ is circular if $w'_{dx} = w'_{dy}$.

In our case, w'_{0x} and w'_{0y} are about 10 μm, while d'_x and d'_y are about 10 mm. Then

$$w'^{\,2}_{0x} \ll \frac{\lambda^2 d'^{\,2}_x}{\pi^2 w'^{\,2}_{0x}}\,, \qquad w'^{\,2}_{0y} \ll \frac{\lambda^2 d'^{\,2}_y}{\pi^2 w'^{\,2}_{0y}}\,, \tag{42}$$

so that $w'_{dx} = w'_{dy}$ and Eqs. (40) and (41) lead to

$$\frac{|d'_x|}{w'_{0x}} = \frac{|d'_y|}{w'_{0y}}\,. \tag{43}$$

There are two solutions for C: one between W'_{0x} and W'_{0y}, the other out of the segment $W'_{0x}W'_{0y}$.

We designed a diffractive lens whose image focal lengths are $f'_x = 19.3\,\text{mm}$ and $f'_y = 10.2\,\text{mm}$. Then we have:

$$w'_{0x} = 14.52\,\mu\text{m}\,, \quad w'_{0y} = 14.85\,\mu\text{m}\,, \quad q'_x = -30\,\mu\text{m}\,, \quad q'_y = -40\,\mu\text{m}\,.$$

Since w'_{0x} and w'_{0y} are very small, if C is between W'_{0x} and W'_{0y} the illuminated area is also very small, and the solution is not acceptable to our purpose. Moreover, approximations of Eq. (42) do not hold (d'_x and d'_y are a few microns long).

If z_c is the distance from the diffractive lens to C, the other solution gives $z_c = 419.5\,\text{mm}$. Considering the irradiance, the transverse radius of the circular area at that distance is 10.02 mm (Fig. 8).

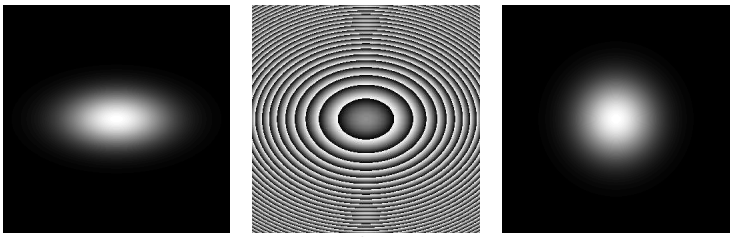

Figure 8. Focusing an astigmatic Gaussian beam on a circular area. (a) Gaussian beam irradiance in the lens plane. (b) Phase levels of the sphero-cylindrical Fresnel lens (represented by grey levels). (c) Irradiance at 30 mm from the lens. (Numerical simulations.)

Finally we consider the source made up of 19 laser diodes. We set a Fresnel lens such as the lens of Fig. 8 in front of each diode (behind a spherical microlens, Fig. 5): the lens is appropriately shifted, so that the illuminated area is the same for every laser diode. Since the 19 laser diodes are incoherent between them, the total irradiance is the sum of the irradiances of the diodes (see Fig. 9).

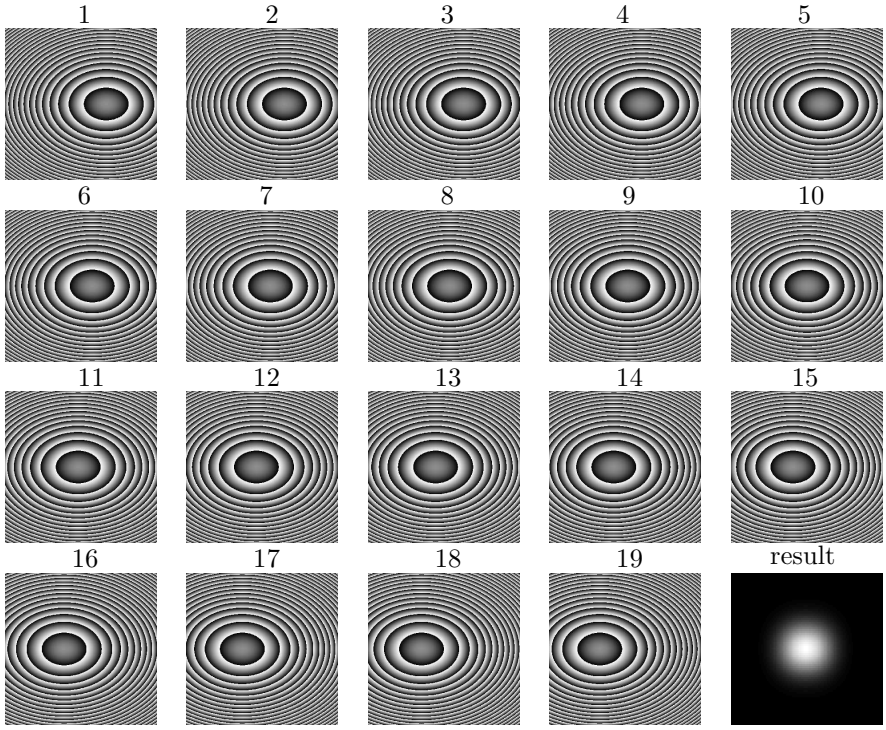

Figure 9. The 19 Fresnel lenses to be set in front of the 19 laser diodes. Each lens is appropriately shifted and produces a circular illuminated area, according to Fig. 8. Botton right: the resulting irradiance in the focus plane.

5. Conclusion

The former study shows that focusing a multi-Gaussian beam source on a unique area is possible by using both refractive and diffractive microlenses. Refractive lenses are necessary because diffractive elements have not a sufficient numerical aperture. Diffractive microlenses are useful because they can be designed to obtaining focal areas with arbitrary shapes.

References

[1] Gao X, Ohashi H, Okamoto H, Takasaka M and Shinoda K 2006 Beam shaping technique for improving the beam quality of a high-power laser-diode stak *Opt. Lett.* **31** 1654–6
[2] Yamaguchi S, Kobayashi T, Saito Y and Chiba K 1997 Collimation of emissions from a 1-cm aperture tightly arranged multistripe laser-diode bar with a multiprism array coupling *Appl. Opt.* **36** 1875–8
[3] Clarkson W A and Hanna D C 1996 Two-mirror beam shaping technique for high-power diode bars *Opt. Lett.* **21** 375–7
[4] Herzig H P 1998 *Micro-optics. Elements, systems and applications* (London: Taylor and Francis)
[5] Zheng G, Du C, Zhou C and Zheng C 2005 Micrograting-array beam-shaping technique for asymmetrical laser beams *Appl. Opt.* **44** 3540–4
[6] Leger J R and Goltsos W C 1992 Geometrical transformation of linear diode-laser arrays for longitudinal pumping of solid-state lasers *IEEE J. Quant. Electron.* **28** 1088
[7] Pellat-Finet P and Bonnet G 1994 Fractional order Fourier transform and Fourier optics *Opt. Comm.* **111** 141–54
[8] Pellat-Finet P 2004 *Lecciones de óptica de Fourier* (Bucaramanga: Ediciones UIS)
[9] Pellat-Finet P 2009 *Optique de Fourier, théorie métaxiale et fractionnaire* (Paris: Springer)
[10] Namias V 1980 The fractional order Fourier transform and its application to quantum mechanics *J. Inst. Maths. Applics* **25** 241–65
[11] McBride A C and Kerr F H 1987 On Namias's fractional Fourier transform *IMA J. Appl. Math.* **39** 159–75

[12] Bonnet G 1978 Introduction à l'optique métaxiale. Première partie : diffraction métaxiale dans un espace homogène : trilogie structurale, dioptre sphérique *Ann. Télécomm.* **33** 143–65
[13] Bonnet G 1978 Introduction à l'optique métaxiale. Deuxième partie : systèmes dioptriques centrés (non diaphragmés et non aberrants) *Ann. Télécomm.* **33** 225–43
[14] Pellat-Finet P and Fogret É 2006 Complex order fractional Fourier transforms and their use in diffraction theory. Application to optical resonators *Opt. Comm.* **258** 103–13.
[15] Torres R, Pellat-Finet P and Torres Y 2006 Sampling theorem for fractional bandlimited signals: A self-contained proof. Application to digital holography *IEEE Signal Process. Lett.* **13** 676–9
[16] Struik D J 1988 *Lectures on classical differential geometry* (New York: Dover)
[17] Pellat-Finet P 1999 Diffraction entre un émetteur et un récepteur localement toriques. Application à l'étude des systèmes astigmates *C. R. Ac. Sc. Paris* **327 IIb** 1269–74